COMMUNICATION

ChemComm
www.rsc.org/chemcomm

Metalloglycomics: a new perspective upon competitive metal–carbohydrate binding using EPR spectroscopy†

Rachel Codd

Centre for Heavy Metals Research, School of Chemistry, University of Sydney, NSW 2006, Australia. E-mail: r.codd@chem.usyd.edu.au; Fax: +61 2 9351 3329; Tel: +61 2 9351 4233

Received (in Cambridge, UK) 27th July 2004, Accepted 4th October 2004
First published as an Advance Article on the web 28th October 2004

Ternary complexes formed between calcium, the oxochromium(v) ion and *N*-acetylneuraminic (sialic) acid (naH_6) of the form, Ca(II)–oxoCr(v)–naH_6, have electronic structures and equilibrium distributions distinct from the binary oxoCr(v)–naH_6 analogues, as illustrated by electron paramagnetic resonance (EPR) spectroscopy.

Sialic acids are a family of carbohydrates ubiquitous throughout the animal kingdom that are structurally defined as 9-membered carbon chains with an α-keto acid head group.[1] The most abundant sialic acid in humans is *N*-acetylneuraminic acid (naH_6; Scheme 1) which occurs predominantly as the terminal residue of protein- and lipid-based cell-surface glycoconjugates.[1] Structural features of naH_6 include a *tert*-2-hydroxycarboxylate 'head' group, which is deprotonated at physiological pH ($pK_a \sim 2.6$), and a glycerol 'tail'. The 2′-OH α-glycoside link from naH_6 to the penultimate glycoconjugate residue orients the glycerol tail towards the extracellular milieu inviting interactions with biometals. The interaction between Ca(II) and naH_6 has been investigated previously;[2] the structure of a binary (1 : 1) complex determined from ^{1}H and ^{13}C NMR spectroscopy (Scheme 1) proposes Ca(II) binds to naH_6 (as the free acid, where $\beta : \alpha \sim 92 : 8$) *via* the carboxylate O^1, O^R, O^7 and O^8 groups.[3]

More recently, both the *tert*-2-hydroxycarboxylate 'head' group of naH_6 (O^1,O^2) in addition to the glycerol 'tail' (O^7,O^8,O^9) have been established as viable chelates of select transition metal ions using electron paramagnetic resonance (EPR) spectroscopy,[4] NMR spectroscopy,[5] or potentiometry;[6] EPR spectroscopy in particular continues to emerge as a powerful tool in studying metal–bioligand speciation.[4,7]

Strong EPR signals from solutions of Cr(VI) and glutathione (GSH) in the presence of excess naH_6 (Fig. 1; black) are attributed to a distribution of five-coordinate oxoCr(v)–naH_6 complexes (d^1) in which two naH_6 units chelate the oxoCr(v) ion ([naH_6] > [oxoCr(v)]) *via* combinations of the O^1,O^2, O^7,O^8 or O^8,O^9 groups.[4] The multiplicity of the central ^{x}Cr ($x = 50, 52, 54$; $I = 0$) signal (Fig. 1; RHS) conveys the number (n) of protons ($I = ½$; $2nI + 1$) in the second coordination sphere that perturb the Cr(v) redox (d_{xy}) orbital (*e.g.*; $n = 0$, bis-O^1,O^2 singlet; $n = 4$, bis-O^7,O^8 quintet; $n = 6$, bis-O^8,O^9 septet).[4] There is a pH dependence of the distribution of oxoCr(v)–naH_6 species whereby isomers of the O^1,O^2-coordinated species ($g_{iso} = 1.9785$; 1.9792) dominate under acidic conditions (Fig. 1a) and the series of O^7,O^8- and O^8, O^9-coordinated species ($g_{iso} \sim 1.9800$) dominate at alkaline pH values (Fig. 1c, d).[4]

This work shows that in the presence of excess Ca(II) ([Ca(II)] : [naH_6] = 10) there is significant modulation to the Cr(v) EPR signals (Fig. 1; purple) which suggests the formation of ternary Ca(II)–oxoCr(v)–naH_6 complexes that have electronic structures (as indicated by variations in g_{iso} values and ^{1}H a_{iso} values) distinct from the binary oxoCr(v)–naH_6 analogues.‡ Also, the pH-dependent equilibrium distribution of oxoCr(v)–naH_6 species clearly differs in the presence of Ca(II); the appearance of complex multiplets at lower pH values in the ternary system, relative to the binary system (Fig. 1b), is likely due to the Ca(II)-induced lowering of the hydroxyl pK_a values of naH_6, thereby increasing the relative concentration of ternary Ca(II)–oxoCr(v)–naH_6(diolato) species. These observations were investigated using EPR simulation procedures.§ The parent Ca(II)–oxoCr(v)–naH_6 signals (at pH values ⩾ 4.49) simulated (correlation > 0.998) as comprising two singlets, two quartets, two septets (Table 1) and up to five additional high-field singlets (present in very low (<3.5%) concentrations at pH values ⩾ 7.14).

Noteworthy differences between the binary oxoCr(v)–naH_6 and ternary Ca(II)–oxoCr(v)–naH_6 systems are as follows. First, the presence of excess Ca(II) appears to mitigate against the formation of oxoCr(v)–naH_6 species involving coordination *via* the O^7,O^8-diolato group, since (unlike the binary system) the simplest simulation model for the Ca(II)–oxoCr(v)–naH_6 system did not

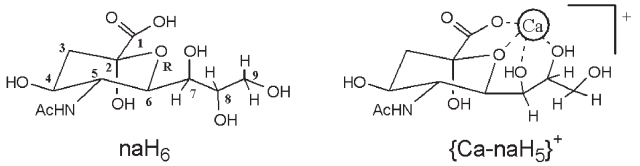

Scheme 1 *N*-Acetylneuraminic acid (naH_6) and Ca(II) complex.[3]

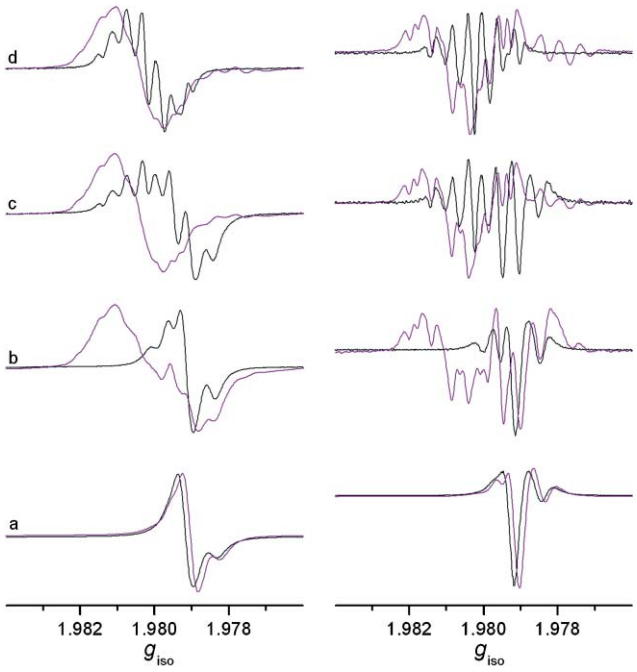

Fig. 1 Room temperature EPR spectra of oxoCr(v)–naH_6 species in the absence (black; pH values: 2.08 (a), 4.37 (b), 7.18 (c), 9.76 (d)) and presence (purple; pH values: 2.13 (a), 4.49 (b), 7.14 (c), 9.62 (d)) of Ca(II) shown as first (LHS) and second (RHS) derivatives of absorption.

† Electronic supplementary information (ESI) available: Parameters from EPR simulation of all spectra shown in Fig. 1. See http://www.rsc.org/suppdata/cc/b4/b411335g/

DOI: 10.1039/b411335g

Table 1 EPR parameters for major Ca(II)–oxoCr(V)–naH$_6$ species

Species	g_{iso}	Multiplicity	^{1}H a_{iso}/H$_{eq}$ [a]	^{1}H a_{iso}/H$_{eq}$ [a]	^{1}H a_{iso}/H$_{eq}$ [a]
CaIa	1.9784	Singlet	N/A [b]	[b]	[b]
CaIb	1.9790	Singlet	[b]	[b]	[b]
CaIIIa	1.9792	Quartet	0.94/1	0.84/1	0.65/1
CaIIIb	1.9794	Quartet	0.96/1	0.83/1	0.58/1
CaVIa	1.9804	Septet	0.98/2	0.79/2	0.58/2
CaVIb	1.9806	Septet	0.95/2	0.73/2	0.54/2

[a] ^{1}H a_{iso} (G); H$_{eq}$ = # magnetically equivalent protons. [b] N/A (singlets).

require the inclusion of a triplet, a quintet or a sextet to model the ternary analogues of $[CrO(O^1,O^2\text{-naH}_4)(O^7,O^8\text{-naH}_3)]^{2-}$ (n = 2), $[CrO(O^7,O^8\text{-naH}_3)_2]^{3-}$ (n = 4) or $[CrO(O^7,O^8\text{-naH}_3)(O^8,O^9\text{-naH}_3)]^{3-}$ (n = 5), respectively. Second, an excellent fit between the experimental and simulated spectra for the Ca(II)–oxoCr(V)–naH$_6$ system was obtained with the inclusion of two isomers each of the singlet, quartet and septet (Table 1). Individual EPR spectra for each species present in the Ca(II)–oxoCr(V)–naH$_6$ equilibrium solution at pH = 4.49 are shown in Fig. 2 (RHS) aligned with the spectra from the related binary oxoCr(V)–naH$_6$ species (LHS) at pH = 4.37. This spectral deconvolution highlights the marked differences in the relative concentrations of related species between the binary oxoCr(V)–naH$_6$ and ternary Ca(II)–oxoCr(V)–naH$_6$ systems (where the absence of a species is represented by a dotted line). The sum of the component spectra (purple) in both the binary oxoCr(V)–naH$_6$ (pH = 4.37) and ternary Ca(II)–oxoCr(V)–naH$_6$ (pH = 4.49) systems closely maps onto the experimental (black) spectrum (Fig. 2; lower trace). In the binary oxoCr(V)–naH$_6$ system, while the presence of two singlets (Fig. 1a) is evident (ascribed to geometrical isomers of $[CrO(O^1,O^2\text{-naH}_4)]^-$ in which donor atoms are juxtaposed about the oxoCr(V) trigonal bipyramid),[4,9] only one isomer is observed (as determined by the limits of EPR simulation) for the remaining linkage isomers. Third, the spectral fit in the Ca(II)–oxoCr(V)–naH$_6$ system required the inclusion of non-uniform ^{1}H a_{iso} values (~0.59 G, 0.80 G, 0.96 G) for second coordination sphere protons within a single species (Table 1). This is distinct from the binary oxoCr(V)–naH$_6$ system, where the conformational flexibility of the glycerol tail of naH$_6$ confers magnetic equivalence upon these protons (^{1}H a_{iso} ~ 0.75 G).

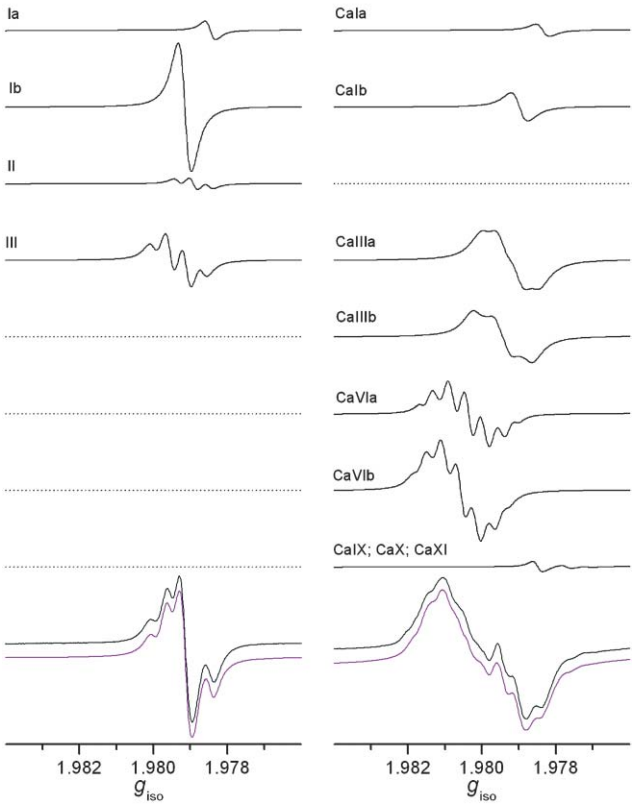

Fig. 2 Simulated EPR spectra for individual oxoCr(V)–naH$_6$ species comprising parent solutions in the absence (LHS; pH = 4.37) and presence (RHS; pH = 4.49) of Ca(II). The addition of simulated spectra (purple) is offset below the experimental spectra (black).

These differences suggest that the interaction between Ca(II) and naH$_6$, as modelled from NMR spectroscopic data (O^1, O^R, O^7, O^8),[3] restricts the conformational flexibility of the glycerol tail, effectively acting as an 'ionic lock'. The ternary Ca(II)–oxoCr(V)–naH$_6$ species (two geometrical isomers each) are assigned (Table 1) as $\{Ca_2[CrO(O^1,O^2\text{-naH}_4)_2]\}^{3+}$ (CaI (a,b)), $\{Ca_2[CrO(O^1,O^2\text{-naH}_4)(O^8,O^9\text{-naH}_3)]\}^{2+}$ (CaIII (a,b); Scheme 2) and $\{Ca_2[CrO(O^8,O^9\text{-naH}_3)_2]\}^{+}$ (CaVI (a,b); Scheme 2). The increase in the strength of the sets of donor atoms (bis-hydroxycarboxylate < hydroxycarboxylate-diolato < bis-diolato) correlates with the increase in the g_{iso} values for CaI (a,b), CaIII (a,b) and CaVI (a,b), respectively, which supports the species assignment, together with the signal multiplicities (Table 1).

The stoichiometry of the ternary Ca(II)–oxoCr(V)–naH$_6$ complexes (2 : 1 : 2) is based upon the known Ca(II) : naH$_6$ stoichiometry (1 : 1) determined from NMR experiments (even where [Ca(II)] > [naH$_6$]),[2,3] and from studies of oxoCr(V)–bioligand systems that show the preferential formation of bis-chelate species (relative to mono-chelate species) where [ligand] : [Cr(V)] ⩾ 2.5.[4,9] The absence of O^7,O^8-coordinated oxoCr(V)–naH$_6$ species in the ternary Ca(II)–oxoCr(V)–naH$_6$ system suggests that the O^7 group of naH$_6$ has a stronger affinity toward Ca(II) than toward the oxoCr(V) ion. Conversely, based upon the presence of O^8,O^9-coordinated Ca(II)–oxoCr(V)–naH$_6$ species, the O^8 group of naH$_6$ has an affinity toward the oxoCr(V) ion (and may be simultaneously binding Ca(II)).

The magnetic inequivalence of the protons in the second coordination sphere of ternary Ca(II)–oxoCr(V)–naH$_6$ complexes (Fig. 2; Table 1) is also explained by the 'ionic lock' mechanism, since the $\{Ca(II)\text{–naH}_5\}^+$ structure places H8, H9 and H9′ in unique magnetic environments.[3] These environments evidently increase the extent of orbital overlap between the second coordination sphere protons and the d_{xy} oxoCr(V) orbital, as measured by the increased ^{1}H a_{iso} values of the Ca(II)–oxoCr(V)–naH$_6$ complexes, relative to the binary oxoCr(V)–naH$_6$ analogues.

Also, there are shifts in g_{iso} values for related species within the binary oxoCr(V)–naH$_6$ and ternary Ca(II)–oxoCr(V)–naH$_6$ systems (Fig. 1). The g_{iso} values of the species involving *tert*-2-hydroxycarboxylate coordination ($[CrO(O^1,O^2\text{-naH}_4)_2]^-$ or $\{Ca_2[CrO(O^1,O^2\text{-naH}_4)_2]\}^{3+}$ in the binary or ternary system, respectively) move to higher field (lower g_{iso}) in the presence of

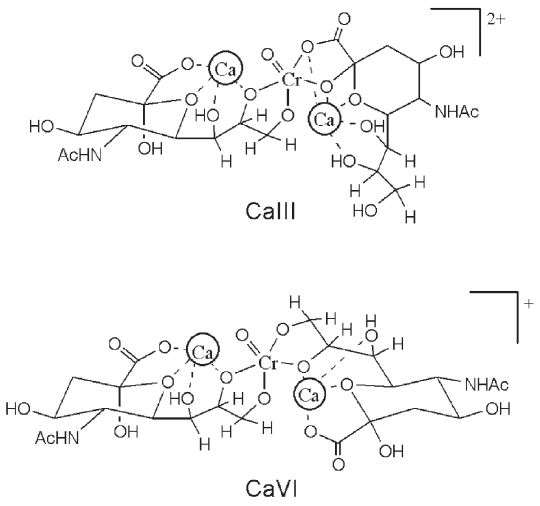

Scheme 2 Proposed Ca(II)–oxoCr(V)–naH$_6$ complexes.

Ca(II), while the g_{iso} values of diolato coordinated species $([CrO(O^8,O^9\text{-}naH_3)_2]^{3-}$ or $\{Ca_2[CrO(O^8,O^9\text{-}naH_3)_2]\}^{+}$ in the binary or ternary system, respectively) move to lower field (higher g_{iso}) in the presence of Ca(II). This latter trend is consistent with $[CrO(glycerol(2-))_2]^{-}$ (g_{iso} = 1.9800), where in the presence of Ca(II), g_{iso} = 1.9803. This suggests that in the case of oxoCr(V)–diolato complexes, the presence of Ca(II) modifies the polarizability of the donor oxygen atom (increases the 'hardness'), which correlates with an increase in the g_{iso} value. No change in g_{iso} value is observed for well characterised *tert*-2-hydroxycarboxylate oxoCr(V) complexes ($[CrO(hmba(2-))_2]^{-}$ (hmba(2−) = 2-hydroxy-2-methylbutanoato), g_{iso} = 1.9784) in the presence of Ca(II), which indicates a poor affinity of Ca(II) towards an isolated hydroxycarboxylate group and suggests that the polyfunctionality of naH_6 is an important determinant of Ca(II) binding.

This is an elegant illustration of the use of EPR spectroscopy in studying competitive metal–carbohydrate binding (termed here 'metalloglycomics') that may have wide ranging implications in understanding transition metal–bioligand speciation in Ca(II)-rich (and/or Mg(II)) matrices that model the biological milieu. The author acknowledges a Sesqui New Staff Support grant and access to the EPR spectroscopy facility at the University of Sydney.

Notes and references

‡ Solutions were prepared from aqueous stock solutions of naH_6, $Na_2Cr_2O_7{\cdot}2H_2O$, $Ca(NO_3)_2$ and GSH with final concentrations of Ca(II), Cr(VI), GSH and naH_6 of 1.0 M, 40 mM, 2 mM and 100 mM, respectively. Under these conditions, $[naH_6] > [oxoCr(V)]$, since the [oxoCr(V)] (formed prior to the ligand-exchange reaction) is dependent upon [GSH] (and $[GSH] < [Cr(VI)]$). The pH values of the solutions were adjusted with aliquots of NaOH prior to being made to volume with water. Under conditions where naH_6 is in excess of [oxoCr(V)–GSH] (*i.e.*; favouring the ligand-exchange reaction), the concentrations of oxoCr(V)–GSH species present are negligible as determined by the absence of oxoCr(V)–GSH signals (g_{iso} = 1.9858 and g_{iso} = 1.996).[8] Although accurate ^{53}Cr A_{iso} values of single species were not clearly resolved due to low signal : noise ratios (particularly in second derivative spectra), an approximate ^{53}Cr A_{iso} value of 17.6 ± 1.0 × 10^{-4} cm^{-1} is able to be determined from the spectrum of the ternary Ca(II)–oxoCr(V)–naH_6 system at pH = 4.49 (data not shown) which is in the range of ^{53}Cr A_{iso} values typical of oxoCr(V)–bis-diolato (16.5 × 10^{-4} cm^{-1}) and –hydroxycarboxylate (17.3 × 10^{-4} cm^{-1}) complexes.[4,9]

§ Continuous wave EPR spectra were recorded at room temperature on a Bruker (EMX) EPR spectrometer at X-band frequency (*ca.* 9.6 GHz), linked to a Bruker field controller (EMX 032T) and gaussmeter (EMX 035M) and simulated using the program WinSIM, developed at the National Institute of Environmental Health Science (available at http://epr.niehs.nih.gov/pest.html). This program fits a simulated isotropic EPR spectrum for up to 10 species (with user defined EPR parameters (g_{iso} (*g* shift), number/type of nuclei, a_{iso} values) to the observed spectrum, using the simplex optimisation algorithm (number of restarts, 4; maximum iterations per restart, 600; fractional tolerance, $n < 0.01$).

1 C. Traving and R. Schauer, *Cell. Mol. Life Sci.*, 1998, **54**, 1330; T. Angata and A. Varki, *Chem. Rev.*, 2002, **102**, 439; A. Rosenberg, *Biology of the Sialic Acids*, Plenum Press, New York, 1995.

2 J.-P. Behr and J.-M. Lehn, *FEBS Lett.*, 1973, **31**, 297; J.-P. Behr and J.-M. Lehn, *FEBS Lett.*, 1972, **22**, 178; L. W. Jaques, B. F. Riesco and W. Weltner, Jr, *Carbohydr. Res.*, 1980, **83**, 21; M. F. Czarniecki and E. R. Thornton, *Biochem. Biophys. Res. Commun.*, 1977, **74**, 553; C. Long and B. Mouat, *Biochem. J.*, 1971, **123**, 829.

3 L. W. Jaques, E. B. Brown, J. M. Barrett, W. S. Brey, Jr and W. Weltner, Jr, *J. Biol. Chem.*, 1977, **252**, 4533.

4 R. Codd and P. A. Lay, *J. Am. Chem. Soc.*, 2001, **123**, 11799; R. Codd and P. A. Lay, *Chem. Res. Toxicol.*, 2003, **7**, 881; R. Codd, J. A. Irwin and P. A. Lay, *Curr. Opin. Chem. Biol.*, 2003, **7**, 213.

5 M. E. Daman and K. Dill, *Carbohydr. Res.*, 1982, **102**, 47.

6 M. Saladini, L. Menabue and E. Ferrari, *J. Inorg. Biochem.*, 2002, **88**, 61.

7 N. V. Nagy, T. Szabó-Plánka, A. Rockenbauer, G. Peintler, I. Nagypál and L. Korecz, *J. Am. Chem. Soc.*, 2003, **125**, 5227.

8 J. Aiyar, K. M. Borges, R. A. Floyd and K. Wetterhahn, *Toxicol. Environ. Chem.*, 1989, **22**, 135; A. Levina, L. Zhang and P. A. Lay, *Inorg. Chem.*, 2003, **42**, 767.

9 R. Bramley, J.-Y. Ji, R. J. Judd and P. A. Lay, *Inorg. Chem.*, 1990, **29**, 3089; R. Bramley, J.-Y. Ji and P. A. Lay, *Inorg. Chem.*, 1991, **30**, 1557; R. Codd and P. A. Lay, *J. Am. Chem. Soc.*, 1999, **121**, 7864.